Full Length Research Paper

The use of confocal microscopy in quantifying changes in membrane potential

Dale Elgar[1]*, Fons Verdonck[2], Anne Grobler[3], Carla Fourie[1], Johan Du Plessis[1]

[1]School for Physiology, Nutrition and Consumer Sciences, North-West University, Private Bag X6001, Potchefstroom, 2520, South Africa.
[2]Interdisciplinary Research Center (IRC), KULAK, B-8500 Kortrijk, Belgium.
[3]School of Pharmacy, North-West University, Private Bag X6001, Potchefstroom, 2520, South Africa.

Monitoring the plasma membrane potential and its changes can be a time consuming and challenging task especially when conventional electrophysiological techniques are used. The use of potentiometric fluorophores, namely tetramethylrhodamine methylester (TMRM), and digital imaging devices (laser scanning confocal microscopy) provides reliable and time efficient method. Two scorpion pore-forming peptides, namely PP and OP1, were used as a tool to induce depolarization of the plasma membrane potential of neuroblastoma cell line and cardiac myocytes. Alternative methods for the neuroblastoma cells and cardiac myocytes were used. Depolarization of the neuroblastoma cells was calibrated with 140 mM KCl solution with 1 μM valinomycin, after which intensity readers were substituted in the Nernst equation for quantification. Calibration of the alternative method used of the cardiac myocytes' plasma membrane potential changes was calibrated with the use of 5, 20, 40, and 80 mM KCl solutions with 1 μM valinomycin. A calibration curve was then constructed from which plasma membrane potential could be calculated.

Key words: Membrane potential, TMRM, potassium concentrations, confocal microscopy, parabutoporin, opistoporin1.

INTRODUCTION

An electrophysiological technique such as current-clamping can be used to measure membrane potential and changes thereof brought about by various factors. This technique is extremely time demanding provided the cells are large enough for the formation of electrode-membrane junctions. The accuracy of this technique is affected by ionic leak currents at the electrode-membrane junction (Ehrenberg et al., 1988; Plášek and Sigler,

―――――――――――――――――
*Corresponding author. E-mail: E-mail: fmsde@puk.ac.za Tel: +27 18 299 2251. Fax: +27 18 299 2248.

Abbreviations: Fluorescence$_{intra}$, intracellular fluorescent intensity; fluorescence$_{intra,}$ extracellular fluorescent intensity; [fluorophores]$_{intra}$, intracellular fluorophores concentration; [fluorophores]$_{extra}$, extracellular fluorophores concentration; $[K_o]$, extracellular potassium concentration; $[K_i]$, intracellular potassium concentration; MP, membrane potential; OP1, opistoporin 1; PP – parabutoproin; and TMRM, tetramethylrhodamine methylester.

1996). The use of potentiometric fluorophores is a fast and accurate way of investigating changes in membrane potential. It provides a means for the measurement of a population of cells' membrane potential thereby improving time efficacy of experimentation as well as the ability to measure the membrane potential of small cells.

TMRM is a fluorophore that alters fluorescence in response to a voltage/potential difference across the cell membrane (Plášek and Sigler, 1996). The potential difference across the cell membrane drives an uneven distribution of TMRM between the intra and extracellular mediums. The cationic nature of TMRM will cause intense fluorescence at more negative membrane potentials, loosing its fluorescence as the membrane potential becomes more positive. Many potentiometric fluorophores bind to the plasma and organelle membranes and have a tendency to aggregate at high fluorophore concentrations. This causes the distribution of the fluorophore to deviate significantly from the Nernst equation (Plášek and Sigler, 1996; Ehrenberg et al.,

1988).

TMRM shows none of these characteristics (Loew et al., 2002) and therefore the fluorophore distribution (concentration) and intensity equilibrates in accordance with the Nernst equation as follows:

$$MP = -60\log\frac{[\text{fluorophore}]_{intra}}{[\text{fluorophore}]_{extra}} = -60\log\frac{\text{fluorescence}_{intra}}{\text{fluorescence}_{extra}}\,mV$$

TMRM is not toxic towards cells and photobleaching does not prove to be a problem (LeMasters et al., 1999).

Scorpion venom contains peptides that target the ion channels (Possani et al., 2000) as well as peptides that target the phospholipids structure of the cell membrane (Verdonck et al., 2000). These membrane-targeting peptides cause the formation of pores in the membrane or total disruption of it. The peptide-induced pores are permeation pathways for ions and the depolarization in neural cells function as a trigger for spontaneous activity and repetitive firing (Verdonck et al., 2000). PP and OP1 are two pore-forming peptides isolated from the southern African scorpion species *Parabuthus schlechteri* Purcell, 1899 (Verdonck et al., 2000) and *Opistophthalmus carinatus* Peters, 1861 (Moerman et al., 2002), respectively. It has been shown that PP depolarizes human granulocytes (Moerman, 2002).

In this study, alternative methods of TMRM and laser scanning confocal microscopy usage were used to quantify plasma membrane potential changes induced by PP and OP1 in SH-SY5Y neuroblastoma cell line and primary rat cardiac myocytes.

MATERIALS AND METHODS

Peptides and chemicals

PP (Swiss-Prot Accession No. P83312) and OP1 (Swiss-Prot Accession No. P83313) were chemically synthesized by Ansynth Service BV (The Netherlands) as described earlier (Moerman et al., 2002). Valinomycin was purchased from Sigma (St. Louis, MO, USA). TMRM was purchased from Molecular Probes (California, CA, USA).

Cellular preparations

SH-SY5Y neuroblastoma cells (ATCC, Virginia, USA) were grown in Dulbecco's modified Eagle's medium (DMEM-F12) and incubated under 5% CO_2 at 37°C. After trypsinization, cells were allowed to adhere to 31 mm circular cover slips placed in 35 mm circular petri dishes containing DMEM-F12 under sterile conditions. Adherence was complete after 5 h.

Primary ventricular cardiac myocytes were isolated from Sprague-Dawley rats (~200 g) using the enzymatic dispersion method developed by Mitra and Morad (1985) and revised by Tytgat (1994). Enzymatic dispersion of the cardiac myocytes was achieved with collagenase, type II (24 mg) and protease, type XIV (4.8 mg) (both purchased from Sigma, St. Louis, MO, USA). Cardiac myocytes were allowed to adhere for 1 h in Tyrode solution ([mM] 137 NaCl, 5.4 KCl, 0.5 MgCl$_2$, 11.6 HEPES, 1.8 CaCl$_2$, 10 glucose, pH 7.4 with NaOH) at room temperature to poly-L-lysine and laminin laminated sterile 31 mm circular cover slips.

TMRM loading

TMRM was added to the Tyrode solution for a final concentration of 0.5 µM. 2 ml of the 0.5 µM TMRM-Tyrode solution was placed in a sterile 35 mm circular petri dish. A cover slip containing adhered neuroblastoma cells or cardiac myocytes was transferred to the petri dish containing the 0.5 µM TMRM-Tyrode solution for 20 min at room temperature (Loew et al., 1998). The cover slip was then removed from the petri dish and placed in a cell chamber. 1 ml of an appropriate solution (discussed further in the Methodology) containing 0.1 µM TMRM was then added to the cell chamber.


Laser scanning confocal microscopy

Digital images of membrane potential changes were captured with a model PCM 2000 confocal microscope (Nikon, Tokyo, Japan) as proposed by Ehrenberg et al. (1988) and Loew et al. (1998). The PCM 2000 was connected to a Nikon (TE300) inverted microscope equipped with a 60x/1.40 Apo Planar oil objective. The system's helium-neon ion laser was used to excite TMRM at 515 nm with emission at 565 nm. A 0% neutral density filter was used to detect mitochondrial membrane potential. The 10% neutral density filter was then used to depict the plasma membrane potential and used throughout the entire imaging process. A pinhole size of 1/4 airy units was used to minimize photobleaching and to obtain a sharper image. The gain was set to ensure the brightest fluorescence (being that of the mitochondria membrane potential) and was < 250 intensity units. The scan rate was 1 frame/s and a total of 8 frames were averaged.

Measuring of membrane potential

Calibration of the neuroblastoma cells were performed in accordance to the method proposed by Loew (1998). 1 ml of a 0.1 µM TMRM-Tyrode solution containing 5.4 mM NaCl and 140 mM KCl with 1 µM valinomycin was added to the cell chamber. The sum of the concentrations of NaCl and KCl should equal that of the normal Tyrode solution. The high extracellular K^+ concentration ($[K_o]$) was used to depolarizes the neuroblastoma cells and the presence of the 1 µM valinomycin brought the plasma membrane potential to the equilibrium potential K^+. This calibration step was performed to compensate for any non-potentiometric binding of TMRM. Cells were monitored for approximately 30 min until the fluorescent intensity of TMRM had reduced and stabilized. At this point the extra and intracellular TMRM fluorescent intensities were measured. The extra to intracellular fluorescent ratio (F_{extra}/F_{intra}) was calculated and used in the Nernst equation to calculate the plasma membrane potential (Figure 1).

The calibration of the cardiac myocytes could not be performed as mentioned above because the cardiac myocytes morphologically altered from a long to spherical shape in the presence of the 140 mM KCl- Tyrode solution. Therefore four different $[K_o]$ were used to calibrate membrane potential in the cardiac myocytes by the calculation of a calibration curve. The circular cover slip was transferred to the cell chamber and 1 ml of a Tyrode solution containing 140 mM NaCl and 5 mM KCl with 1 µM valinomycin was added. As the concentration KCl was increased to 20, 40 and 80 mM, so the concentration NaCl must be reduced to 120, 100, 60 mM, respectively. TMRM fluorescence stabilized after 30 min where after fluorescence was measured to calculate a calibration curve (Figure 2).

Quantification of the neuroblastoma cells' plasma membrane
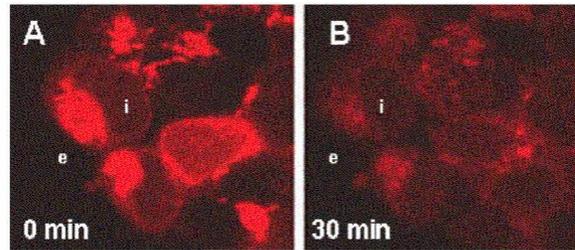
$$e = 5 \text{ IU} \qquad\qquad e = 5 \text{ IU}$$
$$i = 115 \text{ IU} \qquad\qquad i = 25 \text{ IU}$$

Calibration Factor after 30 minutes (F_{extra}/F_{intra})

$$F_{extra}/F_{intra} = 5 \text{ IU} / 25 \text{ IU}$$
$$= 0.2 \perp 0.01$$

$$MP = -60\log\left(\frac{[\text{fluorophore}]_{intra}}{[\text{fluorophore}]_{extra}}\right) = -60\log\frac{\text{fluorescence}_{intra}}{\text{fluorescence}_{extra}} \text{ mV}$$

Resting membrane potential   **Membrane potential after 30 minutes**

$$MP = -60\log\frac{(115*0.2)}{5} = -39.8 \text{ mV} \qquad MP = -60\log\frac{(25*0.2)}{5} = -0.85 \text{ mV}$$

Figure 1. Calculation of changes in depolarizing SH-SY5Y neuroblastoma cells. Effect of high extracellular K^+ (with 1 M valinomycin) on neuroblastoma cells. A bright TMRM fluorescence is representative of the resting membrane potential of each cell (A). After 30 min of exposure to the high extracellular K^+ with valinomycin the fluorescent intensity decreased (B). Calculation of the calibration factor and membrane potential indicated.

potential was performed according to Loew et al. (2000) and LeMasters et al. (1999). After transfer of TMRM loaded cells to the chamber (as mentioned previously), 1 ml of 0.1 µM TMRM-Tyrode solution was added to the chamber. The extra and intracellular TMRM intensities before and after PP or OP1 exposure were captured. The intensities were substituted into the Nernst equation (Figure 1) and used to calculate the plasma membrane potential (Loew et al., 1998). A similar procedure was followed with the cardiac myocytes although the Nernst equation was not used and the plasma membrane potential was extrapolated from the calibration curve (Figure 2).

**Processing of data and statistical significance**

Digital images were analysed with the EZ2000 software (Nikon, Tokyo, Japan). Results were expressed as the mean ± SEM of five repetitions. The significance of the differences was determined using Student's paired and unpaired t-test in Origin, version 5.0 (Microcal Software Inc., © 1991-1997). In all analysis values of $p < 0.05$ were considered statistically significant.

RESULTS

Figures 1A and B shows the reduction of TMRM fluorescence in neuroblastoma cells caused by the 140 mM KCl-induced depolarization in the presence of 1 µM valinomycin. At time 0 min the extracellular intensity was 5 Intensity Units (IU) whereas the intracellular intensity was 115 IU. After 30 min of exposure to the 140 mM KCl

with 1 µM valinomycin solution, the intracellular intensity was reduced to 25 IU with the extracellular intensity being unchanged. Extra and intracellular TMRM intensities were measured at 'e' and 'i' respectively (according to Loew et al., 1998), and the F_{extra}/F_{intra} ratio was calculated to be 0.2 ± 0.01 (n = 5) (Figure 1). The resting membrane potential of the neuroblastoma cells was -38.3 ± 1.9 mV (n = 5) and after 30 min of exposure to the 140 mM KCl

solution (with 1 µM valinomycin) was -0.85 ± 1.5 mV (n = 5) (Figure 1).

Figures 2A and B shows the reduction of TMRM fluorescence in cardiac myocytes caused by the 80 mM KCl-induced depolarization in the presence of 1 µM valinomycin. The intracellular TMRM intensities obtained from exposure to the 5, 20 40 and 80 mM KCl with 1 µM valinomycin solutions were used to construct the grey line (left y-axis) in Figure 2C. The theoretical membrane potentials for each of the four mentioned extracellular K^+ concentrations was calculated with the Nernst equation and plotted as a function of the logarithm of $[K_o]/[K_i]$ (Figure 2 C; black line). The theoretically calculated membrane potentials correlated well with the percentage TMRM fluorescent intensity decrease (r = 0.98). Figure 2D was then calculated where the percentage TMRM fluorescent intensity decrease is expressed as a function of the membrane potential. This graph was used to extrapolate a certain membrane potential for a particular decrease in TMRM fluorescent intensity. The
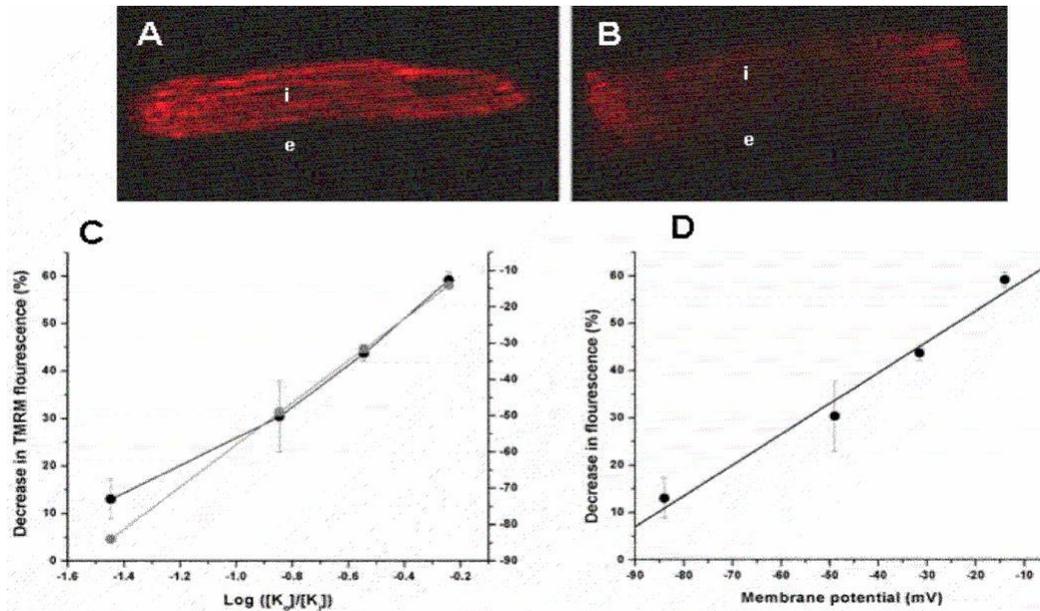
Figure 2. Calculation of changes in depolarizing cardiac myocytes. Cardiac myocytes are shown with a bright TMRM fluorescence indicating a resting membrane potential of each cell (A) and after 30 min of exposure to a 80 mM extracellular K^+ (with 1 M valinomycin) solution (B). (C) The correlation of the decrease in TMRM fluorescence and membrane potential was plotted against the logarithm of $[K_o]/[K_i]$. The grey and black line indicates the measured change in TMRM fluorescence in the presence of the four mentioned $[K_o]$ (left axis) and the membrane potential calculated from the Nernst equation (right axis) respectively. (D) The decrease in TMRM fluorescence was plotted as a function of membrane potential ($r = 0.98$).

resting membrane potential was extrapolated as -83.8 ± 8 mV (n = 5).

The pore-forming nature of PP and OP1 caused depolarization in both cell types (Figure 3). The neuroblastoma cells were depolarized from the resting membrane potential mentioned above to -11.9 ± 3.9 mV (n = 5) and -9.4 ± 1.9 mV (n = 5) by 0.5 M PP and 1-1.5 M OP1, respectively. The cardiac myocytes where also depolarized to -39.7 ± 8.4 mV (n = 5) and -32.6 ± 5.2 mV (n = 5) by 0.5-1 M PP and 1.5-2.5 M OP1. Figure 2 (A-B) and Figure 3 (D-F) indicates that distinguishing between the plasma and mitochondrial membrane potential in the cardiac myocytes was not as distinct as compared to that of the neuroblastoma cells (Figures 3A-B).

DISCUSSION

PP (Verdonck et al., 2000) and OP1 (Moerman et al., 2000) interacts with the membranes of excitable cells, and was used in this study as a pore-forming model to induce the trafficking of ions and depolarization. The method used in determining the changes in membrane potential of the neuroblastoma cells produced results that correspond well with the literature. The resting membrane potential of -38.3 ± 1.9 mV can be supported by the work

of Iwata et al. (1999), Arcangeli et al. (1995) and Higashida et al. (1983) in which whole- cell current clamping was used for membrane potential analysis. A 30 min exposure of the cells to extracellular K^+ solution of 140 mM KCl with 1 µM valinomycin induced a membrane potential of -0.85 ±1.5 mV. This correlates well with the expected membrane potential of 0 mV due equal to K^+ concentrations on either side of the cell membrane (Guyton and Hall, 2000). The use of a range of K^+ concentrations for calculation of a calibration curve provides an alternative method of quantifying membrane potential changes. The resting membrane potential of – 83.8 ± 8 mV corresponds well with results obtained with whole-cell current clamping (Kohmoto et al., 1997). Distinguishing between the plasma and mitochondrial membrane potential in cardiac myocytes proved challenging. This could be due to the dense network of mitochondria distributed throughout cardiac myocytes. This can be observed by the bright fluorescence maintained once certain areas of the cell had lost fluorescence (Figures 3D-F).

It can be concluded that the use of TMRM and laser scanning confocal microscopy along with the two methods discussed allows for time efficient qualitative and quantitative monitoring of membrane potential changes. These methods provide new insights into the monitoring of diseases such as Alzheimer's, in which the
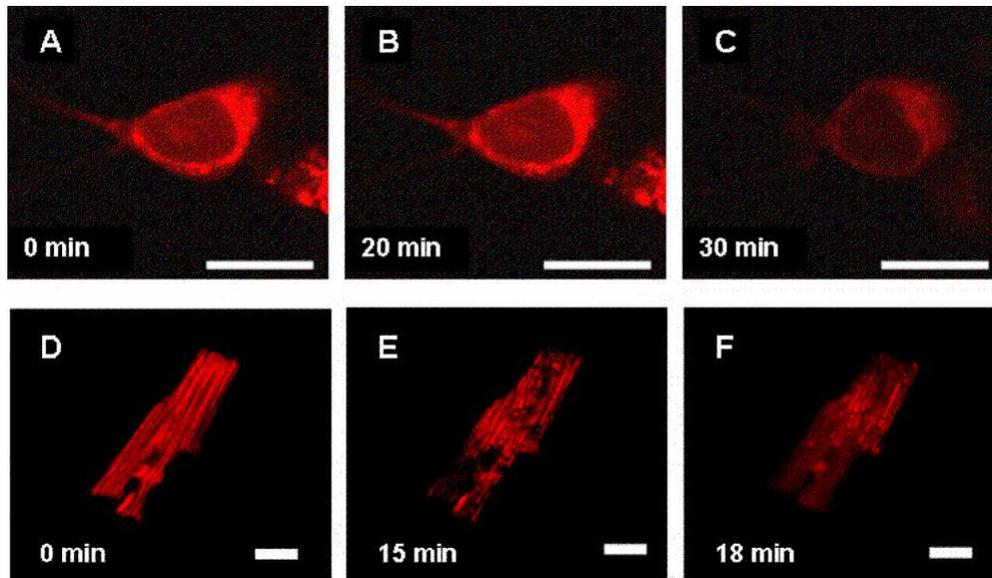
Figure 3. Effect of parabutoporin and opistoporin1 on membrane potential. Confocal microscopy images of TMRM labeled SH-SY5Y neuroblastoma cells (A-C) (bar indicates 10 µm) and cardiac myocytes (D-F) (bar indicates 15 µM) are shown. 0.5 µM PP was administered at time 0 min. The fluorescent intensity of the neuroblastoma cells and cardiac myocytes was reduced by 0.5 µM PP after 30 and 18 min respectively.

pore-forming -amlyoid protein plays a critical role.

REFERENCES

Arcangeli A, Bianchi L, Becchetti A, Faravelli L, Coronnello M, Mini E, Olivotto M, Wanke E (1995). A novel inward-rectifying K^+ current with a cell cycle dependence governs the resting potential of mammalian neuroblastoma cells. J Physiol. 489: 455-471.

Ehrenberg B, Montana V, Wei M, Wuskell JP (1988). Membrane potential can be determined in individual cells from the Nernstian distribution of cationic dyes. Biophys J. 53: 785-794.

Guyton AC, Hall JE (2000). Textbook of Medical Physiology. W.B. Saunders Company, Philidelphia, pp 52-64.

Higashida H, Sugimoto N, Ozutsumi K, Miki N, Matsuda M (1983). Tetanus toxin: a rapid and selective blockage of the calcium, but not sodium, component of action potentials in cultured neuroblastoma N1E-115 cells. Brain Res. 279: 363-368.

Iwata M, Komori S, Unno T, Minamoto N, Ohashi H (1999). Modification of the membrane currents in mouse neuroblastoma cells following infection with rabies virus. Brit J Pharm. 126: 1691-1698.

Kohmoto O, Shimizu T, Sugishita K, Kinugawa K, Takahashi T, Serizawa T (1997). Electivity of felodipine for depolarized ventricular myocytes: a study at the single-cell level. Eur J Pharm. 319: 355-363.

LeMasters JJ, Trollinger DR, Qian T, Casico WE, Ohata H (1999). Confocal imaging of Ca^{2+}, pH, electrical potential, and membrane permeability in single living cells. Methods Enzymol. 302: 341-358.

Loew LM (1998). Measuring membrane potential in single cells with confocal microscope. In Celis (ed) Cell biology: A laboratory handbook, Academic Press, San Diego, pp 139-153.

Loew LM, Campagnola P, Lewis A, Wuskell JP (2002). Confocal and nonlinear optical imaging of potentiometric dyes. Methods Cell Biol. 70: 429-452.

Mitra R, Morad M (1985). A uniform enzymatic method for dissociation of myocytes from the hearts and stomachs of vertebrates. Am J Physiol. 249: H1056-H1060.

Moerman L (2002). Identification and biological activities of -helical, antimicrobial peptides in the venom of scorpions. PhD thesis, Katholieke Universiteit Leuven, Leuven, Belgium.pp. 85-86.

Moerman L, Bosteels S, Noppe W, Willems J, Clynen E, Schoofs L, Thevissen W, Tytgat J, Van Eldere J, van der Walt, JJ, Verdonck, F (2002). Antibacterial and antifungal properties of -helical, cationic peptides in the venom of scorpions from southern Africa. Eur J Biochem 269: 4799-810.

Plášek J, Sigler K (1996). Slow fluorescent indicators of membrane potential: a survey of different approaches to probe response analysis. New Trends Photobiol B: Biol. 33: 101-124.

Possani LD, Merino E, Corona M, Bolivar F, Beccerril B (2000). Peptides and genes coding for scorpion toxins that affect ion-channels. Biochem. 82: 861-868.

Tytgat J (1994). How to isolate cardiac myocytes. Cardiovas Res. 28: 280-283.

Verdonck F, Bosteels S, Desmet J, Moerman L, Noppe W, Willems J, Tytgat J, van der Walt J (2000). A novel class of pore-forming peptides from the venom of *Parabuthus schlechteri* Purcell (Scorpions: Buthidae). Cimbebasia. 16: 247-260.